

Conversion of sustained release omeprazole loaded buccal films into fast dissolving strips using supercritical carbon dioxide (scCO₂) processing, for potential paediatric drug delivery

Sajjad Khan^{1#}, Vivek Trivedi¹, John Mitchell¹, Joshua S. Boateng^{1*#}

¹Department of Pharmaceutical, Chemical & Environmental Sciences, Faculty of Engineering and Science, University of Greenwich at Medway, Central Avenue, Chatham Maritime, ME4 4TB, Kent, UK

*** Correspondence:**

Dr Joshua Boateng (j.s.boateng@gre.ac.uk; joshboat40@gmail.com)

Dr Vivek Trivedi (V.Trivedi@gre.ac.uk)

These authors have made equal contributions to this article

ABSTRACT

This study involves the development of thin oral solvent cast films for the potential delivery of the proton pump inhibitor, omeprazole (OME) *via* the buccal mucosa for paediatric patients. OME containing films were prepared from ethanolic gels (1% w/w) of metolose (MET) with polyethylene glycol (PEG 400) (0.5% w/w) as plasticiser, and L-arg (0.2% w/w) as a stabilizer and dried in an oven at 40°C. The blank and drug loaded films were divided into two groups, one group was subjected to supercritical carbon dioxide (scCO₂) treatment and the other group untreated. The untreated and scCO₂ treated films were then characterised using differential scanning calorimetry, thermogravimetric analysis, scanning electron microscopy, X-ray diffraction, Fourier transform infrared spectroscopy, hydration (swelling), mucoadhesion and *in vitro* drug dissolution studies. Treatment of the solvent cast films with scCO₂ caused significant changes to the functional and physical properties of the MET films. The original drug loaded MET films showed a sustained release of OME (1 hour), whereas scCO₂ treatment of the formulations resulted in fast dissolving films with more than 90% drug release within 15 minutes.

Key Words: Supercritical carbon dioxide, Omeprazole, Metolose, Buccal, Pediatric, fast dissolving film.

Chemical compounds studied in this article

L-arginine; Ethanol; Gelatine; Hydroxypropylmethylcellulose; Methylcellulose; Omeprazole; Polyethylene glycol; Sodium hydroxide.

1 Introduction

There has been a growing interest in the design and development of novel formulations that are age appropriate particularly for paediatric and geriatric patients with swallowing difficulties [Lopez et al., 2015]. Various formulations have been proposed to address this challenge including sublingual tablets, fast disintegrating tablets, buccal films and wafers. These have the advantage of being able to hydrate or dissolve in saliva to release the drug for absorption through the sublingual / buccal mucosa or more easily swallowed when compared to large volumes of liquids or whole tablets. Liu and co-workers in a review discussed the formulation factors affecting the acceptability of traditional oral medicines (e.g. tablets, capsules, liquids) in children including dysphagia (difficulty in swallowing) and flexibility of oral dosage forms. The review concluded that paediatric populations will benefit from novel formulations (including films) that overcome these challenges, such as getting the right formulation for the right age group, taste, smell and palatability. (Liu et al., 2014). In addition, these solid formulations are also suitable for drugs that are unstable in liquid or semi-solid dosage forms. Furthermore, buccal or sublingual absorption avoids gastric acid degradation and hepatic first pass metabolism, which allows administration of lower doses.

A good drug candidate for such application is the proton pump inhibitor omeprazole (5-methoxy-2-[[[4-methoxy-3, 5-dimethyl-2-pyridinyl] methyl] sulfinyl]-1H-benzimidazole) which is an inhibitor of gastric acid secretion. Omeprazole (OME) is an effective short-term treatment for gastric and duodenal ulcers and used in combination with antibiotics for eradication of *Helicobacter pylori* (Stroyer et al., 2006). Its stability in aqueous solution is entirely dependent on the initial pH and, it is rapidly degraded in acidic and neutral conditions but shows greater stability in alkaline medium. We have previously shown the potential of OME based buccal films for sustained delivery via the buccal mucosa for paediatric administration (Khan et al., 2015) and demonstrated the release and permeation of the drug

across pig buccal membrane (Khan et al., 2016). However, though OME is well absorbed from the gastrointestinal tract its oral bioavailability in humans of about 50% which suggests first pass metabolism for this drug. Therefore oral mucosa (buccal / sublingual) absorption combined with residual GIT absorption could constitute a potential approach for improving its oral bioavailability whilst also improving compliance in patients with difficulty in swallowing. Choi and co-workers developed buccal adhesive tablets composed of sodium alginate, HPMC and croscarmellose sodium and loaded with OMEand investigated the buccal permeation of the drug across hamster cheeks. They showed that plasma concentration of OME increased reached a maximum of 370 ng/ml in 45 min after buccal administration with an absolute buccal bioavailability of omeprazole in hamsters of 13.76% (Choi et al., 2000). In another study, permeation of OME incorporated into different Cyclodextrins with and without L-arginine, through pig buccal mucosa was investigated (Figueiras et al., 2009). The showed that the amounts (μg) of drug permeating per cm^2/hour (flux) increased when L-arginine was present, due to its stabilizing effect on the inclusion complex formed. The flux values they reported were OME ($2.382 \mu\text{g}/\text{cm}^2/\text{h}$), OME $_{\beta}\text{CD}$ ($2.685 \mu\text{g}/\text{cm}^2/\text{h}$), OME_MBCD ($3.455 \mu\text{g}/\text{cm}^2/\text{h}$), OME $_{\beta}\text{CD} + \text{Arg}$ ($4.161 \mu\text{g}/\text{cm}^2/\text{h}$), OME_M $\beta\text{CD} + \text{Arg}$ ($5.588 \mu\text{g}/\text{cm}^2/\text{h}$).

Proton pump inhibitors (PPIs) such as OME block the hydrogen/potassium adenosine triphosphatase enzyme situated in the stomach wall thus inhibiting acid secretion, giving relief from ulcers of the oesophagus, stomach and duodenum and from gastro-oesophageal reflux disease (GERD). PPIs change their own chemical formula with the addition of H^+/K^+ adenosine triphosphatase enzyme in the parietal cells, resulting in the formation of active chemical derivative by gaining a proton (H^+), which increases the pH of the stomach and reduces acid secretion from the wall of the stomach. The new protonated chemical compound also possesses the ability to bind with the parietal cells in the stomach wall, thus reducing further acid secretion (Chapman et al., 2011). Therefore systemic action following administration and

absorption across alternative routes such as oral mucosa membranes is possible using appropriate formulations. For example, Widder and co-workers patented unidirectional films and tablets for the delivery of proton pump inhibitor across the oral mucosa (Widder et al., 2004). Mansuri and co in their review, reported that buccal mucoadhesive formulations are potential means delivering PPIs as a means of avoiding degradation in the gastrointestinal tract when administered orally (Mansuri et al., 2016).

In recent years, the application of supercritical fluid technology in formulation development has shown tremendous success in the field of drug delivery (Bruner, 2010; Tabernero et al., 2012). A supercritical fluid (SCF) can be defined as a substance above its critical pressure (P_c) and temperature (T_c) where it exists as a single phase and possesses properties of both liquids and gases (Knez et al, 2015). The liquid-like density of SCF provides solvent power similar to a light hydrocarbon and its gas-like viscosity allows excellent mass transfer and higher diffusivity in a material (Shivonen et al., 1999). A number of different SCFs have been used in various applications such as organic synthesis, cleaning and materials processing [Tabernero et al., 2012; Duarte et al., 2015]. However, carbon dioxide (CO_2) remains the most widely used SCF because of the advantages such as being environmentally benign, non-toxic, non-flammable, non-corrosive, readily available, affordable and easy to remove from the reaction systems in comparison to organic solvents. The low T_c (31.15°C) and P_c (or 73.8 bar) of CO_2 makes it an ideal solvent for the processing of numerous pharmaceutical compounds (Ginty et al., 2005). Supercritical carbon dioxide (scCO_2) is known to be an excellent solvent for numerous low molecular weight non-polar compounds as well as some polar compounds [Mohamed et al., 2011]. It also has good solubility of selected groups of polymers such as amorphous fluoropolymers and silicones [Kendall et al., 1999]. Moreover, scCO_2 is also capable of acting as a swelling or plasticising agent by dissolving in a polymeric matrix (Cooper, 2000).

The applications of SCFs are widely reported for several pharmaceutical operations including crystallisation, micronisation, coating, product sterilisation and drug–cyclodextrin complexation (Rudrangi et al., 2015). Similarly, it has also been successfully applied in the development of thin films and scaffolds (Falk et al., 1997; Yanez et al., 2011; Cooper 2003; Kiran, 2016). Processing with scCO₂ can impart interesting characteristics in thin films and scaffolds in terms of porosity, pore structures and crystallinity. Aydin et al, (2006) synthesised a copolymer of L-lactide and epsilon-caprolactone and used the resultant polymer to prepare composite films. Subsequently, the films were treated with scCO₂ to prepare highly porous sponges for potential use as scaffolds in tissue engineering. They reported that the scaffold pore sizes ranged between 40-80µm and showed that the scCO₂ fabricated scaffolds possessed enhanced cell adhesion, proliferation and differentiation of L929 fibroblast cell line culture. Rinki and co-workers prepared porous chitosan scaffolds for cell culture, by reacting chitin with alkali in the presence of (scCO₂) (Rinki et al., 2009). Composite chitosan-nanohydroxyapatite based scaffolds have also been prepared by means of scCO₂ treatment (Karakeçili & Arıkan, 2012). In their study, nanohydroxyapatite particles were added to acetic acid based chitosan gels which were subsequently frozen, dried with acetone and treated with supercritical fluid which yielded porous scaffolds, with potential for use in bone tissue bio-engineering applications. The application of scCO₂ in the formulation of scaffolds and effect of associated parameters (e.g. pressure and temperature) on such systems are very well reported in the scientific literature but studies on the effect of scCO₂ processing on thin films for drug delivery purposes are scanty.

The aim of this study was to investigate the effect of scCO₂ processing on blank (BLK) and drug loaded (DL MET) films and compare their properties with the non-treated films. The films (both scCO₂ treated and non-treated) have been functionally characterised for their

surface morphology, water content, physico-chemical (crystalline/amorphous nature; physical interactions), hydration (swelling), adhesive and OME dissolution properties.

2 Materials and Methods

2.1 Materials

Metolose (MET) was obtained as a gift from Shin Etsu (Stevenage, UK), polyethylene glycol (PEG 400), L-arginine (L-arg) and gelatine were all obtained from Sigma-Aldrich (Gillingham, UK). Ethanol, potassium dihydrogen phosphate and sodium hydroxide were purchased from Fisher Scientific (Leicester, UK) while Omeprazole (OME) was obtained from TCI (Tokyo, Japan).

2.2 Methods

2.2.1 Formulation (gel and film) development

Preliminary 1% w/w gels were prepared by adding the required weight of polymer (MET) to the relevant solvent (20% v/v ethanol) at room temperature. The polymeric gel was heated to 40°C following complete hydration. Based on the total weight of polymer, the plasticiser (PEG) was added to obtain 0.5% w/w concentrations in the final gel. The resultant gel was cooled to room temperature and left stirring on a water bath for 30 minutes to achieve a homogeneous dispersion and then left overnight to remove all entrapped air bubbles.

Once a clear homogeneous gel was obtained, 20g was gently poured into Petri dishes (86mm diameter) and kept in a pre-heated oven at 60°C for 24 hours. The dried films were then carefully peeled off from the Petri dish and photographs taken using a digital camera. Films were then sealed in poly bags and placed in a desiccator over silica gel at room temperature until required.

2.2.2 Formulation of OME loaded films

The OME-loaded films were obtained by initially preparing MET gels as described above. However, the drug was added to the appropriate volume of 20% v/v ethanol to form an OME solution (0.1% w/w). Due to the breakdown of OME following gel formation, L-arg was used as a stabilising agent to prevent drug degradation. This step was performed by adding L-arg (0.20% w/w) to the drug solution keeping the original OME concentration (0.10% w/w) constant. The polymer was then added slowly to the vigorously stirred OME-L-arg drug solution at room temperature to obtain the drug loaded gels and PEG added. The resulting gels were covered with parafilm and left overnight to allow air bubbles to escape, then 20g was poured into Petri dishes and dried at 40°C.

2.2.3 scCO₂ processing of thin films

Supercritical carbon dioxide (scCO₂) treatment of the films was carried out on a Thar Technology Inc instrument containing a 150ml high pressure vessel. BLK and DL films were cut into 2cm² strips and placed in a glass vial. The vial containing the thin film was placed in the high pressure vessel preheated to 40°C. The CO₂ was then introduced into the chamber and pressure was slowly increased to 100 bar. These chosen conditions were mild and also allowed desired miscibility between scCO₂, ethanol and water required for successful drying of thin films studied in this work (Brunner, 2010; Quiño et al., 2016). The system was allowed to equilibrate for 15 minutes once the required pressure was achieved. The CO₂ pump was stopped and the chamber was depressurized at a rate of 7g/min with the help of automated back pressure regulator (ABPR). After complete depressurisation, the sample was removed from the high pressure vessel, digitally photographed and stored in poly bags and placed in a desiccator over silica gel at room temperature until required for further investigations.

2.2.4 Differential scanning calorimetry (DSC)

DSC was used to characterise the thermal behaviour of the films and changes in their properties with introduction of PEG and drug. Analysis of the films and starting materials were carried out on a Q2000 (TA Instruments) calorimeter. About 2.5mg of each sample was placed into hermetically sealed Tzero aluminium pans with a pin hole in the lid and heated from -40°C to 180°C at a heating rate of 10°C/min under constant purge of nitrogen (100mL/min).

2.2.5 Thermogravimetric analysis (TGA)

TGA studies were performed using a Q5000 (TA Instruments) thermogravimetric analyser. About 1-2.5mg of films (BLK and DL) was placed into hermetically sealed Tzero aluminium pans with a pin hole in the lid. Samples were heated under nitrogen atmosphere at a flow rate of 25ml/min from ambient temperature to 600°C at a heating rate of 2°C/min.

2.2.6 Scanning electron microscopy (SEM)

SEM was used to investigate the surface morphology of the films and to check for film uniformity and the presence of any cracks. The films were analysed using a Hitachi Triple detector CFE-SEM SU8030, (Roland Schmidt, Hitachi High-Technologies Europe, Germany) scanning electron microscope. Films were mounted onto Agar Scientific G301 aluminium pin-type stubs (12mm diameter) with Agar Scientific G3347N double-sided adhesive carbon tapes and chrome coated (Sputter Coater S150B, 15nm thickness). The coated films were analysed at accelerating voltage of 2kV.

2.2.7 X-ray diffraction (XRD)

XRD was used to investigate the physical form (crystalline or amorphous) of the films (BLK and DL). XRD patterns of films and starting materials were obtained with a DIFFRAC plus

instrument (Bruker Coventry, UK) equipped with an XRD commander programme. A Goebel mirror was used as monochromator which produced a focused monochromatic CuK α _{1&2} primary beam ($\lambda=1.54184\text{\AA}$) with exit slits of 0.6mm and a Lynx eye detector for performing the experiment. The operating conditions during the experiment were 40kV and 40mA. Film samples were prepared by cutting into 2cm² square strips, mounted on the sample cell and scanned between 2 theta of 0° to 70° and counting time of 0.1 second step size.

2.2.8 Attenuated total reflectance (ATR) Fourier transform infrared (ATRFT-IR) spectroscopy

FT-IR spectra were obtained using a Spectrum Two Perkin Elmer spectrophotometer (Perkin Elmer, US) equipped with a crystal diamond universal ATR sampling accessory (UATR).

Before each measurement, the ATR crystal was carefully cleaned with ethanol. During the measurement, the sample was in contact with the universal diamond ATR top-plate. For each sample, the spectrum represented an average of 4 scans recorded in the range 4000-400cm⁻¹.

2.2.9 Hydration behaviour

The hydration (swelling) capacities of the formulated (BLK and DL films were determined by incubating the samples in 10mL of 0.01M PBS solution (pH 6.8 ± 0.1 simulating salivary pH) set at 37 ± 0.1°C. The buffer solution was prepared by dissolving 6.8g of potassium dihydrogen phosphate in 1L of deionised water and adjusting the pH to 6.8 using sodium hydroxide (NaOH). The films were cut into 2cm² strips and placed into small Petri-dish containing 10mL of the media (PBS) and initially weighed. At predetermined time intervals of 5 minutes the liquid media was removed using a syringe and weighed again. Before the films were weighed excess buffer solution was blotted off with tissue. After weight had been recorded, 10mL of fresh buffer solution was placed back in the Petri dish using a syringe. These studies were

performed in triplicate ($n = 3$) for each set of formulated samples and average values were calculated.

The swelling capacity determined by calculating the swelling index (%) using the equation below:

$$\text{Swelling Index (\%)} = \frac{W_s - W}{W} \times 100$$

Where W_s is the weight of the film after hydration and W is the initial weight of the film after before hydration.

2.2.10 Mucoadhesion

The *in vitro* mucoadhesion experiments were performed for BLK and DL films with a TA HD plus Texture Analyser (Stable Micro Systems, Surrey, UK) fitted with a 5kg load cell. The film was attached to an adhesive rig probe (75mm diameter) with double sided adhesive tape. An 88mm diameter Petri dish was used containing 20g gelatine solution (6.67% w/w) allowed to set as a solid gel and the surface of the gel was equilibrated with 0.5mL of PBS (pH 6.8) to represent the buccal mucosa surface and saliva conditions (Kianfar et al., 2014). The texture analyser was set to tensile mode and the probe set to approach the model buccal mucosal surface with set parameters for adhesivity using the following settings: pre-test speed 0.5mm/s; test speed 0.5mm/s; post-test speed 1.0mm/s; applied force 1N; contact time 60.0 seconds; trigger type auto; trigger force 0.05N and return distance of 10.0mm. Texture Exponent 32 software was used to record and process the data. The peak adhesive force (PAF) required to separate the film from the mucosal surface was determined by the maximum force. The area under the curve (AUC) representing the total work of adhesion (TWA) was estimated from the

force-distance plot whiles the cohesiveness of the sample was determined by the distance of travel.

2.2.11 *In vitro* release of OME using Franz-type diffusion cell

Before the dissolution studies, drug assay and uniformity of OME within the film was determined. This was measured by weighing the film accurately to 5mg ($n=3$) and hydrated in 8ml of drug dissolution media (0.01M PBS pH 6.8 at 37°C). The hydrated film was stirred at $37 \pm 0.5^\circ\text{C}$ until completely dissolved. The concentration of OME was analysed using HPLC.

In vitro drug dissolution studies were carried out using Franz-type diffusion cells. 5mg of MET DL film was placed in the donor compartment on stainless steel wire mesh which separated the donor and receiver compartments, with the mucoadhesive surface in contact with the wire mesh and facing the receiver compartment of the Franz diffusion cell (Cui et al., 2008). The receiver chamber was filled with 8mL of 0.01M PBS pH 6.8 at 37°C with magnetic stirring at a speed of 250 rev/min. The chambers were held together by a cell clamp and sealed with parafilm, in order to limit evaporation and the temperature of the diffusion cell was maintained at $37 \pm 0.5^\circ\text{C}$ and stirred throughout the experiment. Though bicarbonate is the major buffering agent in saliva, we employed phosphate buffer as we previously used simulated saliva based on a previously published work which employed sodium dihydrogen phosphate and therefore we had to use PBS to compare with behaviour in the simulated saliva to allow consistency of buffer ions present.

Aliquots (1mL) of the dissolution medium was sampled at predetermined time intervals and replaced with the same amount of fresh medium to maintain a constant volume for 2 hours. The sampled dissolution medium was measured using HPLC as described below. The concentration of OME released from the film was determined by interpolation from the linearized calibration curve ($R^2 > 0.99$) and cumulative percentage drug release profiles plotted.

The dissolution profiles were further compared using the time to release 20% of the drug ($t_{20\%}$) and the mean percentage release at 15 minutes ($t_{15\text{min}}$).

2.2.12 HPLC analysis

Concentration of DL films as well as drug release in dissolution studies were analysed using an Agilent 1200 HPLC equipped with an auto sampler (Agilent Technologies, Cheshire, UK,) with a Chemstation® software program. The stationary phase used was a Hypersil™ ODS C18 HPLC column, 5 μm particle size (250 x 4.6mm) (Thermo Scientific, Hampshire UK). The mobile phase consisted of a mixture of ammonium acetate and acetonitrile in the ratio of 60:40v/v. The flow rate of the mobile phase was maintained at 2ml/min and detector wavelength for OME was set at 302nm respectively. 20 μl volumes were injected during each run. Standards from 10-50 $\mu\text{g}/\text{ml}$ were used to plot calibration curves for OME ($R^2 > 0.99$).

3 Results

3.1 Supercritical fluid (CO₂) treated films

Figure 1 shows the visual appearance of both BLK and DL films before and after treatment with scCO₂. The preliminary observation of the formulated films (BLK and DL) treated in scCO₂, showed a slight difference in the colour, texture and apparent physical strength of the scCO₂ treated films compared to the untreated films. The scCO₂ treated BLK films showed a rough surface whereas DL films were slightly yellow in colour and more opaque compared to the non-treated films.

3.2 Differential scanning calorimetry (DSC)

Figures 2a and 2b respectively show the DSC thermograms of BLK and DL MET films treated with scCO₂ compared with non-scCO₂ treated original films. In Figure 2a the thermogram of

scCO₂ treated BLK film was characterised by a broader endothermic peak at 56.57°C, and no definite melt or glass transition peaks was obtained and was similar to that of non-treated BLK film which showed a peak at 56.67°C. The thermograms presented in Figure 2b for DL film treated in scCO₂ also showed a broad endothermic peak at 63.31°C, followed by another endothermic peak at 133.49°C, indicating the melting of possibly recrystallized OME. This observation was different from the non-treated DL film which showed a broad peak at 83.41°C, followed by another endothermic peak at 151.82°C which could represent depressed melting point of trace amounts of crystalline OME whilst the rest largely remained amorphous.

3.3 Thermogravimetric analysis (TGA)

TGA was used to determine the equilibrium residual moisture content (%) of both the scCO₂ treated and untreated BLK and DL MET films. As seen in table 1 the highest percent moisture content was observed in scCO₂ treated DL MET film at 5.91% which was higher than non-scCO₂ treated DL MET film (5.14%). However, in the case scCO₂ treated BLK MET film, the reverse was true with a residual moisture content of 3.16% which was again higher than the non-scCO₂ treated films (1.99%) and the difference was statistically significant ($p < 0.05$).

Table 1 TGA results showing weight loss observed for DL MET films from ethanolic (20 % v/v EtOH), PEG 400 (0.5 % w/w) gels containing OME: L-arg (1:2) treated with and without scCO₂.

Films	Weight loss (%)
BLK MET film (non- scCO ₂ treated)	1.99
BLK MET film (scCO ₂ treated)	3.16
DL MET film (non-scCO ₂ treated)	5.14
DL MET film (scCO ₂ treated)	5.91

3.4 Scanning electron microscopy (SEM)

The surface morphology and topographic characteristics of BLK and DL MET films were evaluated using SEM. Figures 3a and 3b show micrographs of the pure OME and L-arg. Figure 3c shows rough and lumpy surfaces for scCO₂ treated BLK film compared to the untreated BLK film (data not shown). Micrographs obtained for DL films treated with scCO₂ (Figure 3d) also had rough surface with presence of crystals compared to the untreated DL film (data not shown) which was smooth and homogenous.

3.5 X-ray diffraction (XRD)

XRD analysis was performed to determine the crystalline - amorphous ratio and confirm the physical form of the various components within the films. Figures 4a and 4b, show the XRD diffractograms of BLK and DL films with and without scCO₂ treatment. The results clearly suggest that there is no difference between the BLK films treated with scCO₂ and non-treated equivalent, whilst DL MET films treated with scCO₂ showed 5% crystallinity compared to non-treated film which was completely amorphous. Figures 5a and 5b show the XRD-diffractograms for the pure starting materials and their physical mixtures respectively. XRD diffractograms for the pure starting materials showed that MET and PEG 400 were amorphous in nature whilst OME and L-arg were highly crystalline.

3.6 ATR- (FT-IR) spectroscopy

Figures 6a and 6b show the FT-IR spectra for BLK and DL MET films treated with and without scCO₂. There were differences observed in the FTIR profiles of scCO₂ treated films compared to non-scCO₂ films as evident from the major peaks listed in tables 2 and 3. Some of the main peaks disappeared whilst others shifted to higher wavenumber and in some cases new peaks appeared that were not originally present in the corresponding non-treated film. In the case of

the BLK films (table 2), all the peaks present in the non-treated films were also present in the scCO₂ treated films, however, two unique peaks appeared at 1314.06 and 1642.42cm⁻¹ for the scCO₂ treated films, which were completely absent in the non-treated films. For the DL films, a different observation was made in that unique peaks were observed in both the scCO₂ treated and non-treated films (table 3). The non-treated DL films showed two peaks at 1059.40 and 1204.25cm⁻¹ which were completely absent in the corresponding scCO₂ treated films, whilst the scCO₂ treated DL films showed three peaks at 1310.40, 1375.02 and 1453.21cm⁻¹ that were completely absent in the non-treated equivalent. Further, the three unique peaks in the scCO₂ treated DL films were also absent in the scCO₂ treated BLK films.

Table 2 Comparing and contrasting the major FTIR peaks of interests for plasticised BLK MET films showing effect of scCO₂. The main peaks present in scCO₂ treated films but missing from the non-treated films are highlighted in bold font.

Non- scCO ₂ treated			scCO ₂ treated		
Peak No.	cm ⁻¹	%T	Peak No.	cm ⁻¹	%T
1	3436.89	82.77	1	3445.31	86.97
2	2876.04	78.65	2	2899.32	84.70
3	-	-	3	1642.42	93.99
4	1454.96	84.38	4	1454.86	86.28
5	1349.02	82.95	5	1374.15	83.93
6	-		6	1314.06	86.33
7	1057.70	24.61	7	1053.56	27.98
8	944.92	58.75	8	944.97	60.73

Table 3 Comparing and contrasting the major FTIR peaks of interests for DL MET films. The main peaks present in scCO₂ treated films but missing from the non-treated films and vice versa are highlighted in bold font.

Non- scCO ₂ treated			scCO ₂ treated		
Peak No.	cm ⁻¹	%T	Peak No.	cm ⁻¹	%T
1	3436.11	87.32	1	3374.27	85.32
2	2877.31	83.30	2	2926.33	82.47
3	1628.42	80.65	3	1630.45	78.84
4	1554.01	81.28	4	1561.06	79.46
5	-	-	5	1453.21	78.15
6	1406.59	81.93	6	1404.00	78.84
7	1204.25	82.33	7	1375.02	77.62
8	-	-	8	1310.40	80.89
9	1059.40	49.64	9	1055.37	34.88
10	945.33	72.55	10	945.78	65.01

3.7 Hydration (swelling) capacity

The untreated BLK and DL MET films showed a swelling index of 1841% and 2630% respectively in 20 minutes. In the case of scCO₂ treated films, there was not enough time to weigh the swollen gel to calculate percent swelling index for the films as they disintegrated within seconds (25 seconds for BLK films and 40 seconds for DL films) of coming in contact with the PBS (pH 6.8).

3.8 Mucoadhesion

The mucoadhesion results (Figures 7a and 7b) show that in all cases, the non-treated BLK and DL films recorded higher adhesive values (cohesiveness, PAF and TWA) than the scCO₂ treated films.

3.9 *In vitro* release of OME using Franz-type diffusion cell

Figure 8 shows the dissolution profiles of scCO₂ treated and non-treated DL MET films in PBS (pH 6.8). The scCO₂ treated DL film showed higher cumulative release (94% in 10 minutes) than non- treated DL films (70% in 60 minutes).

3.10 Comparison of release profiles

In this study, the time to release 20% of the drug ($t_{20\%}$) and the percentage cumulative release at 15 minutes ($t_{15\text{min}}$) were used to compare the DL scCO₂ treated and non-treated films (Costa et al, 2001) and results are shown in table 4. The results showed that scCO₂ treated DL film released 20% of OME within 0.6 minutes whereas non-treated scCO₂ DL film took 5.5 minutes to release the same percentage of the drug. Further, within 15 minutes, non-treated DL film released up to 55% and whilst scCO₂treated DL film released 92% of drug which is a significant difference ($p < 0.05$)

Table 4 A comparison of the time to release 20% of drug ($t_{20\%}$) and the amount of drug released after 15 minutes ($t_{15\text{ min}}$) from both scCO₂ treated and non-treated DL MET films.

DL MET films	Time to release 20% of drug ($t_{20\%}$)	Mean % release at 15 min ($t_{15\text{min}}$)
Non-treated	5.5	55
scCO ₂ treated	0.6	92

4 Discussion

In the current study, the effect of scCO₂ treatment on the functional physico-chemical properties of solvent cast buccal films incorporating OME for paediatric drug delivery were investigated.

The DSC peak at 56.57°C and 63.31°C, can be attributed to evaporation of water and therefore possible that the scCO₂ treated films absorbed some moisture during sample preparation for DSC analysis due to the highly dried nature. The endothermic peak at 133.49°C, suggests possibly recrystallized OME. However, the actual melting point of OME is 158°C (Khan et al., 2015) and therefore this peak could represent either a polymorphic form or a eutectic peak arising from combining L-arg and OME. The treatment with scCO₂ seems to have enhanced the ease with which water molecules are removed (hence lower dehydration temperature) and also seems to have resulted in OME with lower melting points. The higher residual water in scCO₂ treated films is interesting as it suggests that the equilibrium residual moisture content of scCO₂ treated films is dependent on the drug (OME) content and possibly also affected by L-arg since this was required to stabilize OME in the DL films. The scCO₂ process appears to have generated a film matrix that allows rapid evaporation of residual moisture, through the preservation of the swollen structures (Gin et al., 2009). To confirm the observed crystals as recrystallized drug, SEM and XRD was used.

The differences in surface topography could be attributed to CO₂ entering the film matrix and drying the film by removing trapped solvent and causing some of the drug to molecularly dispersed drug to recrystallize on the film surface (Lan et al., 2011). The 5% crystallinity of DL MET film treated in scCO₂ in Figure 4b (2-theta peak 9° and 24°) correspond to the XRD peaks of OME as shown in Figures 5a and 5b (Khan et al., 2015) for the pure drug and physical mixtures respectively. This confirms the DSC and SEM results which suggests possible recrystallization of a small amount of the molecularly dispersed OME present in the original

DL films. Further, the XRD diffractogram for the physical mixture of the four starting materials (OME, L-arg, PEG400 and MET) contains peaks found in all the pure starting materials, implying very little interaction in the physical mixtures, unlike the case of DL films, where most of the components were largely amorphous, with the exception of the small amounts of OME which appeared crystalline after scCO₂ treatment.

The various unique IR peaks observed for the different films analysed indicated that the physical property of both BLK and DL loaded films did change via new physical and chemical interactions between the main components (i.e. polymer and PEG for BLK films and polymer, PEG, OME and L-arg for DL films) with scCO₂ treatment. It further confirms the hypothesis that scCO₂ treatment is able to significantly alter performance characteristics of thin films by altering the functional physico-chemical properties.

The significant changes in hydration properties of the films with scCO₂ treatment is expected to impact on the drug release characteristics of the treated films once in contact with saliva. The main step of scCO₂ consists of the anomalous swelling of polymer thin films caused by scCO₂ within the film matrix. This could be due to the fact that scCO₂ dried these films in a far more efficient manner and the resulting films were most probably more porous than the original ones. They fell apart as soon as they came in contact with water as they were ‘charged’ to have a high affinity for water due to a higher specific surface area (Li et al., 2007; Pham et al., 2003).

The reduced mucoadhesion of the treated films is can be explained by the swelling results discussed above. In the case of the non-treated films, the formulations hydrated more slowly and formed a swollen gel without disintegrating, which allowed formation of stronger physical interactions between the swollen polymer (MET) and the model mucosa (gelatine gel) surface. In the case of the scCO₂ treated films, the rapid hydration and eventual disintegration of the hydrated matrix will have quickly formed a low viscosity gel which flows easily and

therefore had weaker interaction and shorter contact time with the surface of the gelatine gel. This is interesting and can be explained by the diffusion theory of mucoadhesion where the initial swelling stage is necessary to allow for inter-molecular diffusion between the polymeric chains and that of the mucosa surface to consolidate adhesive forces. However, if this initial hydration and swelling is too rapid, it results in the formation of a slippery mucilage which is less adhesive (Ayensu et al., 2012; Pawar et al., 2014).

The higher cumulative release in scCO₂ treated DL film is related to rapid disintegration as observed in the hydration (swelling) data. The slower release of OME from the non-treated film could be attributed to the initial swelling of the polymeric network of MET over a longer period to form a more viscous gel which controls the diffusion of drug into the dissolution medium. It is also interesting to note that unlike the non-treated films, which showed a sustained release profile, the scCO₂ treated films showed two phases of release. The first phase up to 10 minutes released a total of 94% before it plateaued in the second phase. The different phases suggests different mechanisms may be at play during dissolution most likely a combination of drug diffusion and erosion/disintegration which eventually ‘dumps’ most of the drug into the medium. The comparison of release profiles goes to confirm the conversion of a relatively slower release formulation to rapid disintegration film after treatment with scCO₂.

In previous studies (Khan et al., 2015, 2016), we developed mucoadhesive and sustained release MET based films incorporating OME as a model drug and L-arg as stabilising agent to prevent drug degradation. Functional characterisation showed release of the drug and subsequent permeation through pig buccal tissues over a two hour period, owing to prolonged retention at the buccal mucosa surface. Different studies report a residence time and ideal release period ranging from 2 – 6 hours (Choi et al., 2000; Figueiras et al., 2009; Khan et al., 2015; Trastullo et al., 2016) with the maximum usually between 4 – 6 hours. We opted for the lower time period of 2 hours (Khan et al., 2015, 2016), taking into consideration the expected difficulty of retaining formulations in the buccal region of paediatric patients for prolonged periods, for example challenges such as feeding and tongue movements. This study has shown that treatment of the sustained release films with scCO₂ changed them into rapid release formulations as observed in the results above.

Overall, the lower adhesion on the model buccal mucosa and higher *in vitro* release profile of the scCO₂ treated formulations could contribute to concentration of the free drug in saliva within a short period of time. For buccal films intended for only buccal mucosa delivery, the ideal situation is for the drug to be concentrated in the buccal mucosa in a time compatible with its absorption, which was relatively short in the case of the treated films. This could result in a situation where all the rapidly released drug is not completely absorbed across the buccal mucosa. As a consequence, some of the drug present in the saliva will be absorbed in other regions such as sublingual and GIT after swallowing. However, a study by Choi and Kim (2000) investigating the absorption of OME across human oral cavity, they showed that about 23% of the administered dose was absorbed from the oral cavity in 15 min after the administration of OME solutions. Therefore, though a significant amount of OME was released from the scCO₂ treated films, within 30 minutes, it is still possible that enough

could be absorbed across the buccal mucosa and sublingual route to elicit the desired systemic therapeutic action.

In a recent study, Chonkar and co-workers developed fast dissolving HPMC based buccal films incorporating nanoparticles loaded with lercanidipine and showed high dissolution rates and improved ex-vivo permeation through porcine buccal mucosa (Chonkar et al., 2016). Haque and Sheela (2015), developed polymer-bound fast dissolving buccal films of chitosan containing different disintegrating agents, for buccal delivery of metformin hydrochloride. They showed that disintegration time was less than 30 minutes for all formulations, attributed to the effect of the disintegrants. The optimum formulation combining sodium starch glycolate and microcrystalline cellulose, released 92.2% within 6 minutes which was deemed appropriate for rapid absorption across the buccal mucosa. A buccal mucoadhesive fast dissolving film was developed using pullulan as the main component and physically evaluated for moisture content, disintegration time, and mucoadhesion. The films showed respective values 14%, 41.6 seconds and 40 kg/cm² for moisture content, disintegration time and mucoadhesive force, which were deemed appropriate (Vila et al., 2014). These values were not too different from that obtained in the current study.

Further, given that it can be challenging for a younger paediatric patient to hold a film in the buccal region long enough, whilst some find it difficult to swallow significant amounts of liquid formulations due to possible vomiting, use of rapid disintegrating films of OME combining both oral mucosa (buccal, sublingual) and GIT absorption appear to be will be a feasible approach to paediatric delivery of OME. In addition, the volume of hydration and dissolution medium used to hydrate the films at a given time point, is significantly higher than that produced by a normal paediatric patient, and therefore it will be expected to hydrate and release drug more slowly *in vivo*.

5 Conclusion

The results show that scCO₂ caused significant changes to the physical properties and functional performance characteristics of the MET films and converted the original DL MET films from a sustained release formulation to a fast dissolving drug release system, releasing > 90% of OME within 15 minutes. Therefore, scCO₂ drying can offer real opportunities for the formulation of fast dissolving thin films with the potential for paediatric buccal administration and subsequently easily swallowed with little difficulty. Though the release within 15 minutes is short, this could prove ideal for children with swallowing difficulties, by the combination of buccal absorption initially, followed by GIT absorption upon swallowing of non-absorbed portion.

5 References

- Aydin, H.M., Turk, M., Calimli, A., Piskin, E., 2006. Attachment and growth of fibroblasts on poly(L-lactide / ϵ -caprolactone) scaffolds prepared in supercritical CO₂ and modified by polyethylene imine grafting with ethylene diamine-plasma in a glow-discharge apparatus. *The Int. J. Artif. Org.* 29(9), 873-880.
- Ayensu, I., Mitchell, J.C., Boateng, J.S., 2012. Effect of membrane dialysis on characteristics of lyophilised chitosan wafers for potential buccal delivery of proteins. *Int. J. Biol. Macromol.* 50, 905-909.
- Brunner, G., 2010. Applications of supercritical fluids. *Annual Rev. Chem. Biomol. Eng.* 1, 321-42.
- Chapman, B., Rees, C., Lippert, D., Sataloff, R., 2011. Adverse Effects of Long-Term Proton Pump Inhibitor Use: A Review for the Otolaryngologist. *J. Voice*, 25(2) 236-240.
- Choi HG, Kim CK. 2000. Development of omeprazole buccal adhesive tablets with stability enhancement in human saliva. *J. Contr. Rel.* 68 (3), 397-404.
- [Choi H¹](#), [Jung J](#), [Yong CS](#), [Rhee C](#), [Lee M](#), [Han J](#), [Park K](#), [Kim C](#). 2000. Formulation and in vivo evaluation of omeprazole buccal adhesive tablet. *J. Contr. Rel.* 68(3), 405–412.
- Chonkar, A.D., Rao, J.V., Managuli, R.S., Mutalik, S., Dengale, S., Jain, P., Udupa, N. 2016. Development of fast dissolving oral films containing lercanidipine HCl nanoparticles in semicrystalline polymeric matrix for enhanced dissolution and ex vivo permeation *Eur. J. Pharm. Biopharm.* 103, 179-191.
- Cooper, A.I., 2000. *J. Mater. Chem.* 10, 207-234.
- Cotsa, P., Lobo, J.M.S., 2001. Modeling and comparison of dissolution profiles. *Eur. J. Pharm. Sci.* 3 (2), 123-133.

Cui, F., He, C., He, M., Cui, T., Yin, L., Qian, F., Yin, C., 2008. Preparation and evaluation of chitosan-ethylenediaminetetraacetic acid hydrogel films for the mucoadhesive transbuccal delivery of insulin. *J. Biomed. Mater. Res. Part A*, 1064-1071.

Duarte, A.R.C., Mano, J.F., Reis, R.L., 2015. *Polymer Processing Using Supercritical Fluid-Based Technologies for Drug Delivery and Tissue Engineering Applications*. Taylor & Francis group, Pan Stanford.

Falk, R., Randolph, T.M., Meyer, J.D., Kelly, R.M., 1997. Controlled Release of ionic compound from poly (L-Lactide) microspheres produced by precipitation with a compressed anti-solvent. *J. Contr. Rel.* 44 (1) 77.

Figueiras, A., Hombach, J., Veiga, F., Bernkop-Schnürch, A. 2009. In vitro evaluation of natural and methylated cyclodextrins as buccal permeation enhancing system for omeprazole delivery. *Eur. J. Pharm. Biopharm.* 71(2), 339–345.

Fu, Y., Kao, W.J., 2010. Drug release Kinetics and transport mechanisms of non-degradable polymeric delivery system. *Expert Opin. Drug Deliv.* 7(4): 429-444.

Gin, P., Asada, M., Endoh, M.K., Gedelian, C., Lu, T.M., Koga, T., 2009. Introduction of molecular scale porosity into semicrystalline polymer thin films using supercritical carbon dioxide. *Appl. Phys. Lett.* 94, 121908.

Ginty, P., Whittaker, M., Shakesheff, K., Howdle, S., 2005. Drug Delivery goes supercritical. *Mater. Today.* 8(8), 42-48.

Haque, S.E., Sheela, A. 2015. Development of polymer-bound fast-dissolving metformin buccal film with disintegrants, *Int. J. Nanomed.* 10, 199-205.

Karakeçili, A., Arıkan, A., 2012. Preparation of chitosan-nanohydroxyapatite composite scaffolds by a supercritical CO₂ assisted process. *Polym. Comp.* 33(7) 1215-1223.

Kendall, J.L., Canelas, D.A., Young, J.L., Desimone, J.M., 1999. Polymerization in supercritical carbon dioxide. *Chem. Rev.* 99 (2), 543 - 564.

Khan, S., Trivedi, V., Boateng, J.S. 2016. Functional physico-chemical, *ex vivo* permeation and cell viability characterization of omeprazole loaded buccal films for paediatric drug delivery. *Int. J. Pharm.* 500 (1-2), 217–226.

Khan, S., Boateng, J.S., Mitchell, J., Trivedi, V., 2015. Formulation, Characterisation and Stabilisation of Buccal Films for Paediatric Drug Delivery of Omeprazole. AAPS PharmSciTech DOI 10.1208/s12249-014-0268-7.

Kianfar, F., Ayensu, I., Boateng, J.S., 2014. Development and physico-mechanical characterization of carrageenan and poloxamer based lyophilized matrix as a potential buccal drug delivery system. *Drug Dev. Ind Pharm.* 40(3), 361-369.

Kiran, E., 2016. Supercritical fluids and polymers – The year in review – 2014. *The J Supercrit. Fluids.* 110, 126–153.

Knez, Z., Hrncic, M.K., Skerget, M., 2015. Particle Formation and Product Formulation Using Supercritical Fluids. *Annual Rev. Chem. Biomol. Eng.* 6, 379-407.

Lan, Q., Yu, J., Zhang, J., He, J., 2011. Enhanced crystallization of Bisphenol a polycarbonate in thin and ultrathin films by supercritical carbon dioxide. *ACS Publications.* 44, 5743-5749.

Li, Y., Park, E.J., Lim, K.T., Johnston, K.P., Green, P.F., 2007. Role of interfacial interactions on the anomalous swelling of polymer thin films in supercritical carbon dioxide. *Wiley Inter Science.* 45, 1313-1324.

Lui, F., Rammal, S., Batchelor, H.K., Orlu-Gul, M., Ernest, T.B., Thomas, I.W., Flanagan, T., Tuleu, C. 2014. Patient-Centred Pharmaceutical Design to Improve Acceptability of Medicines: Similarities and Differences in Paediatric and Geriatric Populations. *Drugs.* 74(16), 1871–1889.

Lopez, F.L., Ernest, T.B., Tuleu, C., Gul, M.O., 2015. Formulation approaches to pediatric oral drug delivery: benefits and limitations of current platforms. *Expert Opin. Drug Deliv.* 12(11): 1727–1740.

- Mansuri, N.S., Parejiva, P.B., Soniwala, M.M., 2016. Glimpse of drug delivery systems for proton pump inhibitors. *Int. J. Pharm. Sci. Rev. Res.* 36(1), 81-88.
- Mohamed, A., Eastoe, J., 2011. How can we use carbon dioxide as a solvent? *Contemp. Topics Sch. Sci.* 93, 73 - 80.
- Pawar, H.V., Boateng, J.S., Ayensu, I., Tetteh, J., 2014. Multi functional medicated lyophilised wafer dressing for effective chronic wound healing. *J. Pharm. Sci.* 103(6) 1720 - 1733.
- Pham, V.Q., Rao, N., Ober, C.K., 2003. Swelling and dissolution rate measurement of polymers thin films in supercritical carbon dioxide. *The J. Supercrit. Fluid.* 31, 323-328.
- Quiño, J., Ruehl, M., Klima, T., Ruiz, F., Will, S., Braeuer, A., 2016. Supercritical drying of aerogel: *In situ* analysis of concentration profiles inside the gel and derivation of the effective binary diffusion coefficient using Raman spectroscopy. *The J. Supercrit. Fluid.* 108, 1–12.
- Rinki, K., Tripathi, S., Dutta, P.K., Dutta, J., Hunt, A.J., Macquarrie, D.J., Clark, J.H., 2009. Direct chitosan scaffold formation *via* chitin whiskers by a supercritical carbon dioxide method: a green approach. *J. Mater. Chem.* 19, 8651-8655.
- Rudrangi, S.R.S., Trivedi, V., Mitchell, J.C., Wicks, S.R., Alexander, B.D., 2015. Preparation of olanzapine and methyl- β -cyclodextrin complexes using a single-step, organic solvent-free supercritical fluid process: An approach to enhance the solubility and dissolution properties. *Int. J. Pharm.* 494(1), 408-416.
- Shivonen, M., Jarvenpaa, E., Hietaniemi, V., Huopalathi, R., 1999. Advances in supercritical carbon dioxide technologies. *Trends Food Sci. Tech.* 10, 217-222.
- Tabernero, A., del Valle, E.M., Galán, M.A., 2012. Supercritical fluids for pharmaceutical particle engineering: Methods, basic fundamentals and modelling. *Chem. Eng. Proc.* 60:9–25.

Trastullo, R., Abruzzo, A., Saladini, B., Gallucci, M.C., Cerchiara, T., Luppi B., Bigucci, F., 2016. Design and evaluation of buccal films as paediatric dosage form for transmucosal delivery of ondansetron. *Eur. J. Pharm. Biopharm.* 105, 115-121.

Vila, M.M.D.C., Tardelli, E.R., Chaud, M.V., Tubino, M., Balcão, V.M. 2014. Development of a buccal mucoadhesive film for fast dissolution: Mathematical rationale, production and physicochemical characterization, *Drug Del.* 21 (7), 530-539.

Yañez, F., Martikainen, L., Braga, M.E., Alvarez-Lorenzo, C., Concheiro, A., Duarte C.M., Gil, M.H., de Sousa, H.C., 2011. Supercritical fluid-assisted preparation of imprinted contact lenses for drug delivery. *Acta Biomater.* 7(3); 1019-30.

Widder, K., Hall, W., Olmstead, K., 2004. Transmucosal delivery of proton pump inhibitors US Patent. 20040006111 A1.

FIGURE LEGENDS

Figure 1 Digital images showing physical appearance of (a) non-treated BLK films, (b) non-treated DL films, (c) scCO₂ treated BLK films (d) scCO₂ treated DL films.

Figure 2 DSC thermograms of (a) scCO₂ treated and non-treated BLK MET films and (b) scCO₂ treated and non-treated DL MET films.

Figure 3 SEM micrographs of (a) pure OME (b) pure L-arg, (c) scCO₂ treated BLK films and (d) sCO₂ treated DL films.

Figure 4 XRD diffractograms for (a) BLK films and (b) DL films with and without scCO₂ treatment.

Figure 5 (a) XRD diffractograms for the pure MET, OME, L-arg and PEG 400 and (b) XRD diffractogram of physical mixture comprising film formulation components (MET, OME, L-arg and PEG 400)

Figure 6 FT-IR spectra of (a) BLK films with and without scCO₂ treatment and (b) DL films with and without scCO₂ treatment.

Figure 7 *In-vitro* mucoadhesion profiles of (a) BLK film and (b) DL film with and without scCO₂ treatment (mean \pm SD, $n = 3$).

Figure 8 Drug dissolution profiles showing cumulative percent release against time of OME from both scCO₂ treated and untreated DL films (mean \pm SD, $n = 3$).

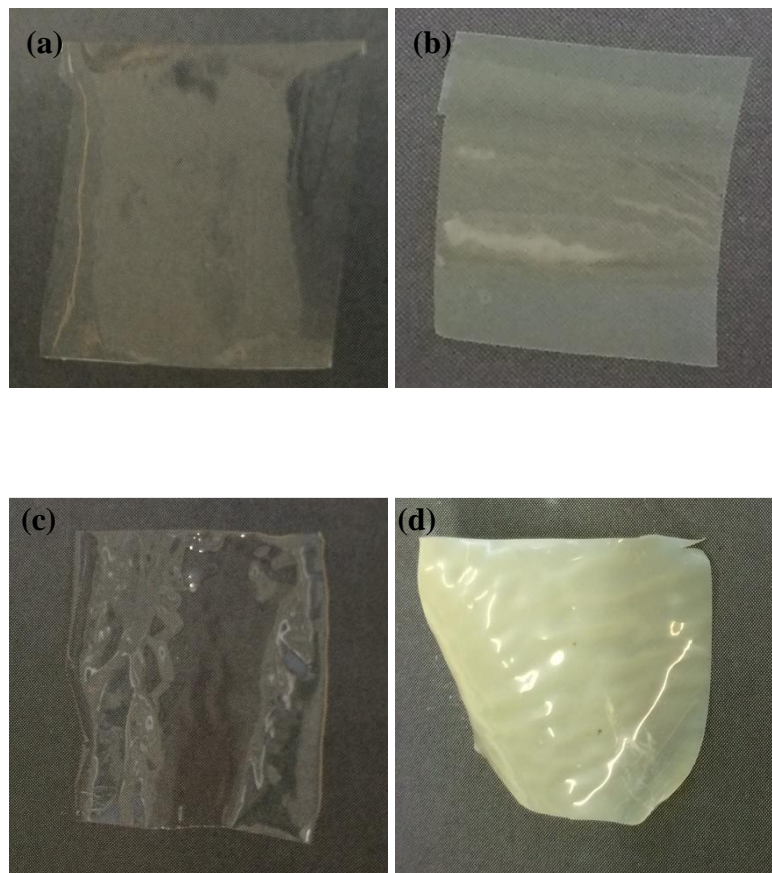
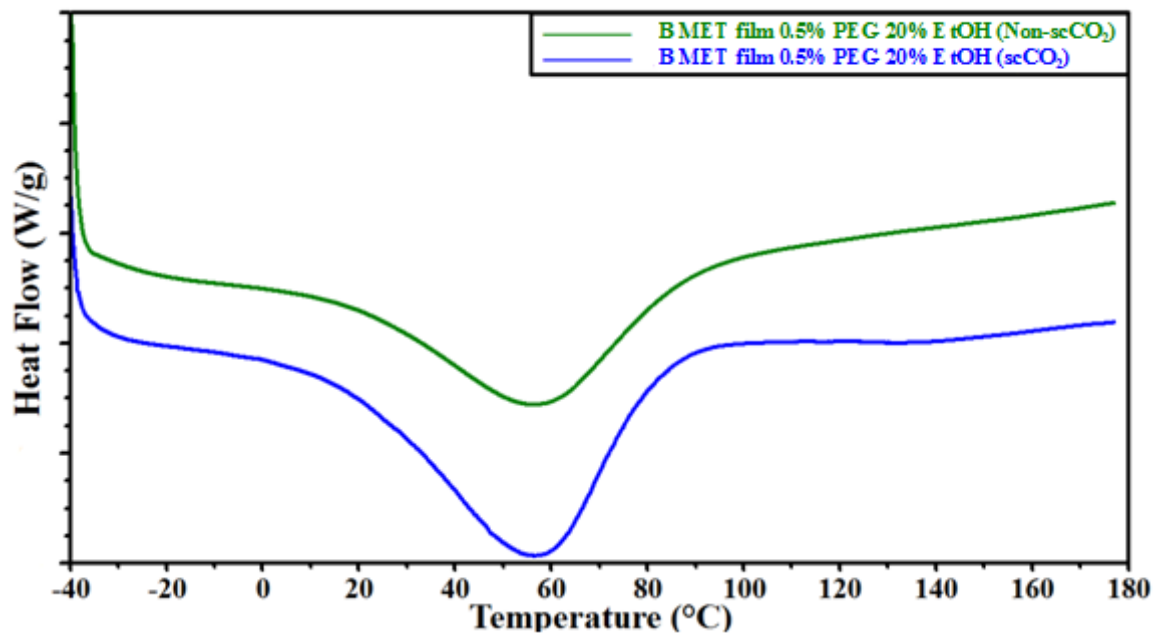
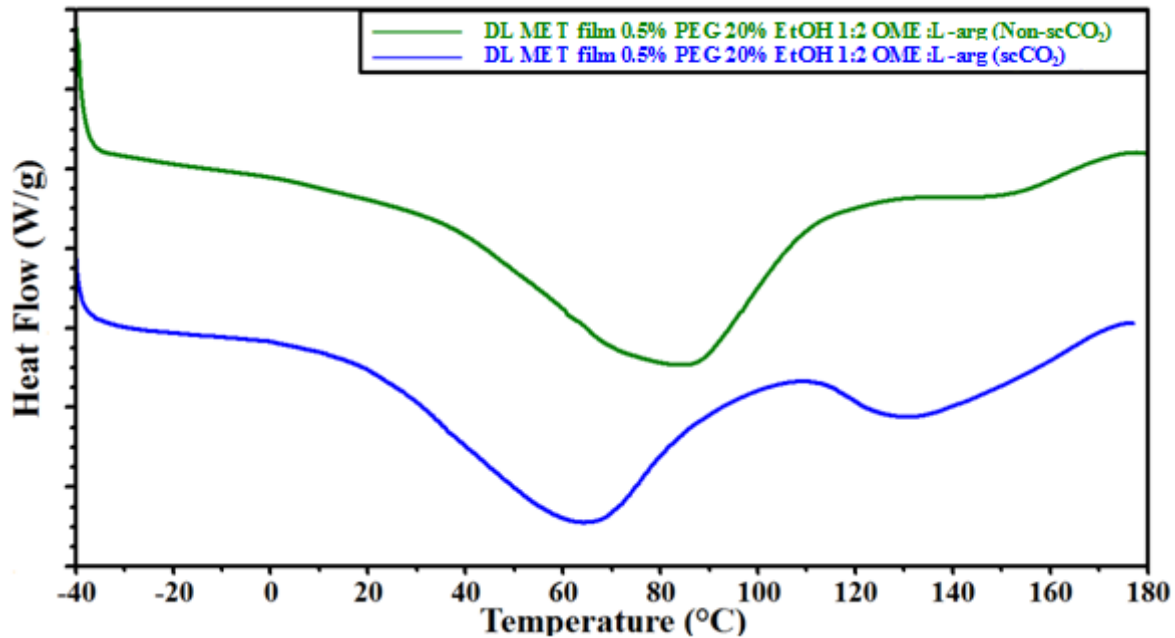


Figure 1

For colour online and print in black and white



(a)



(b)

Figure 2

For colour online and print in black and white

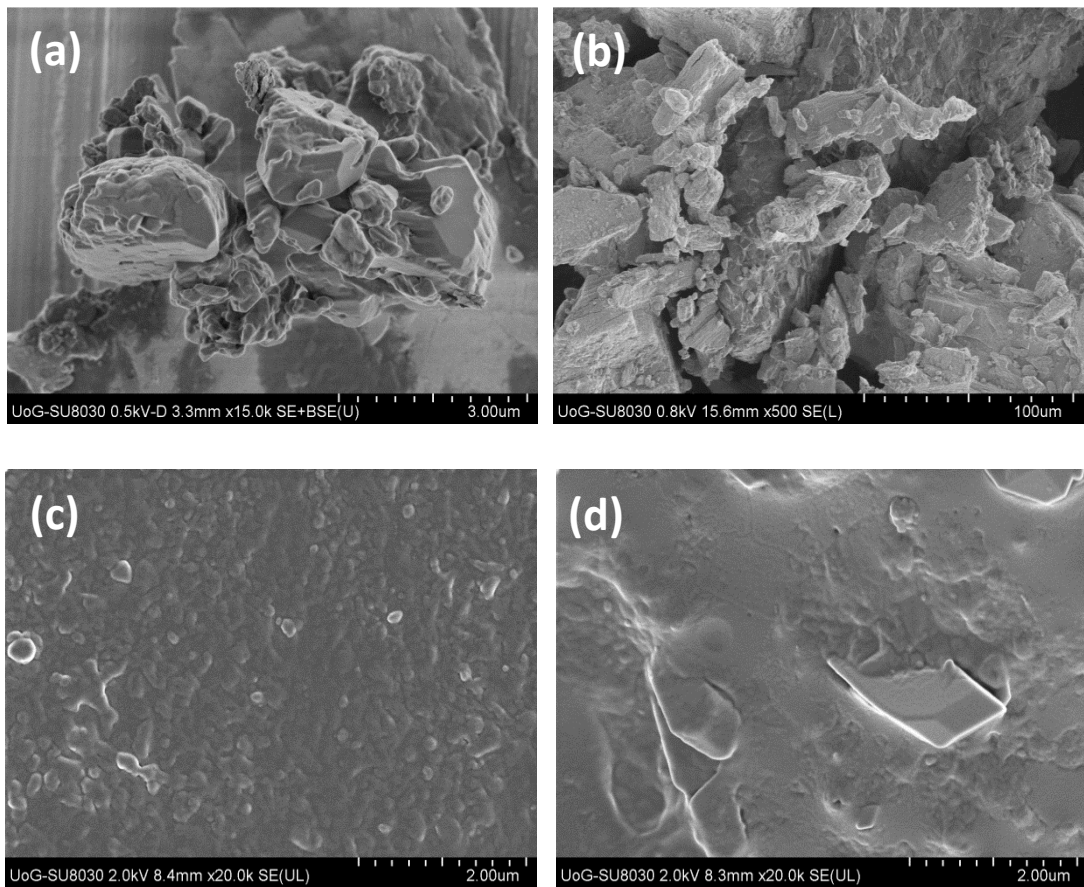
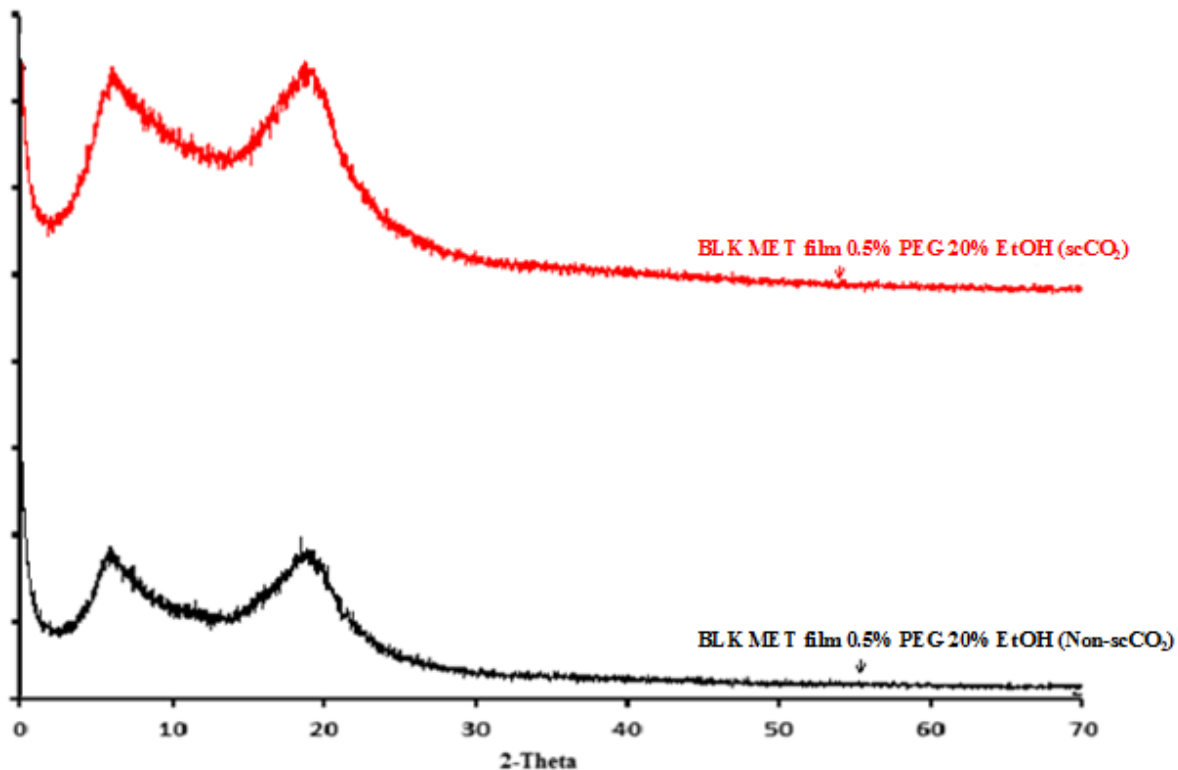
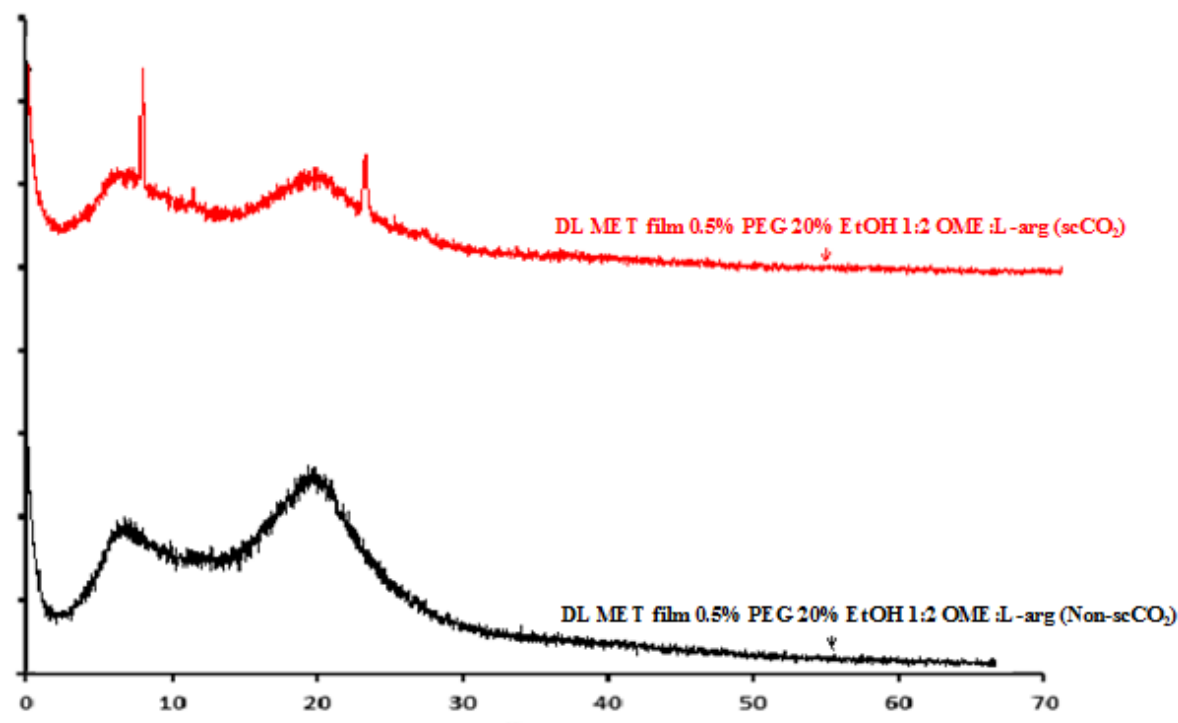


Figure 3



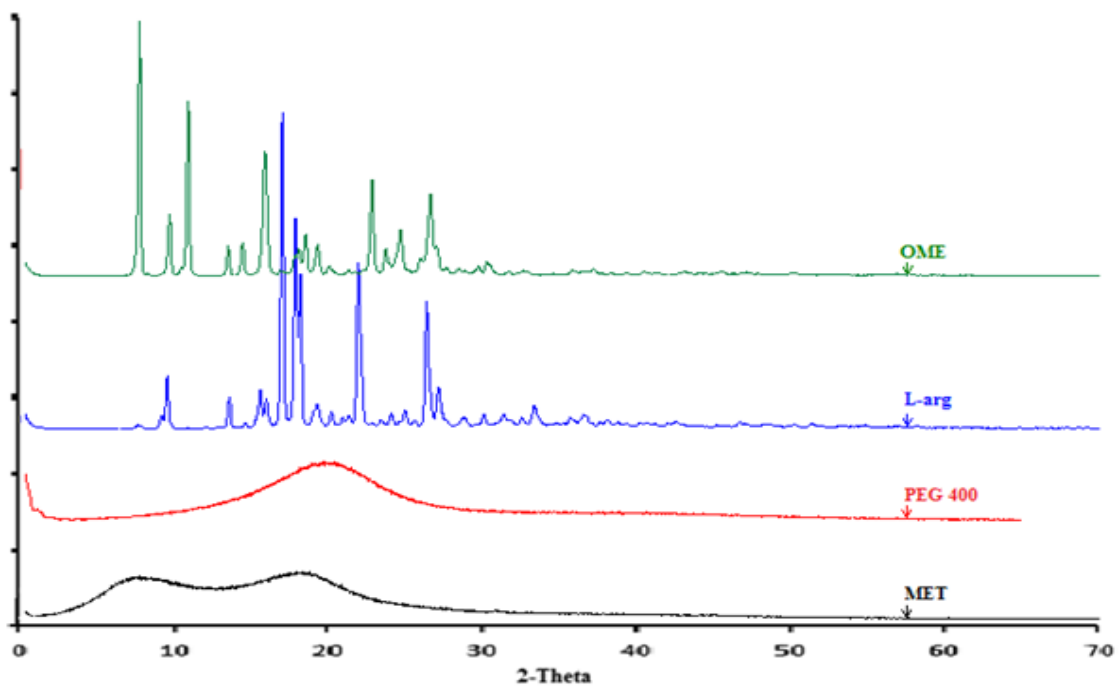
(a)



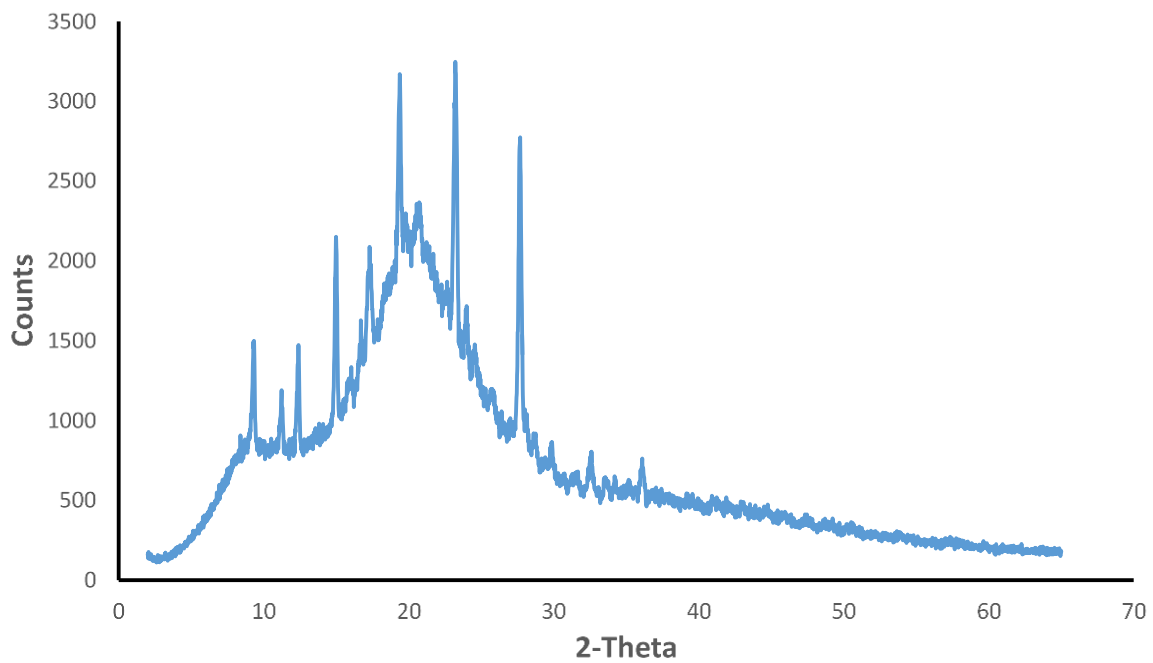
(b)

Figure 4

For colour online and print in black and white

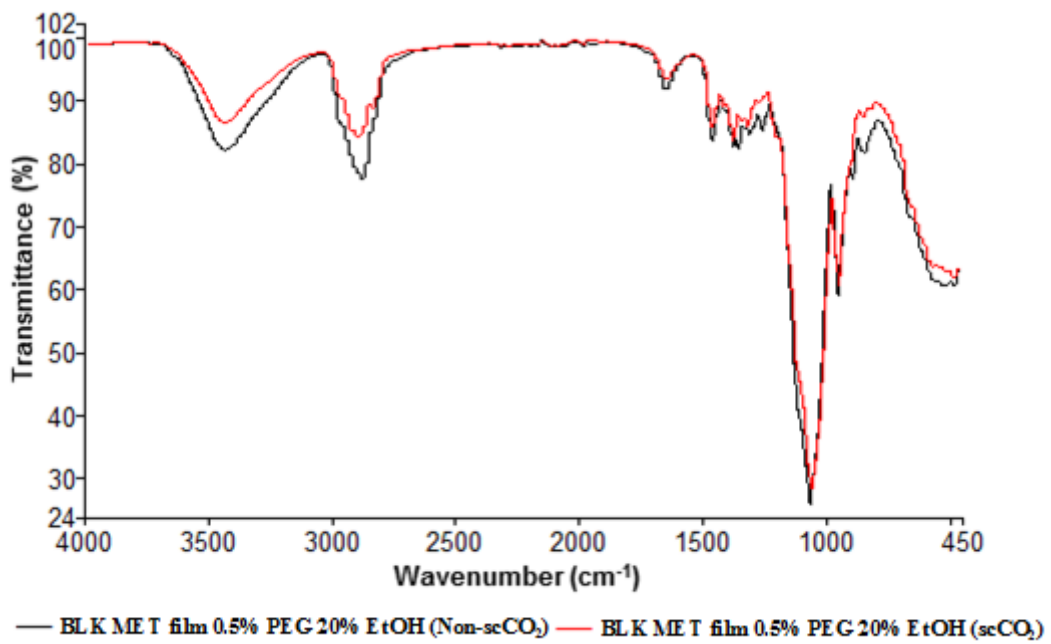


(a)

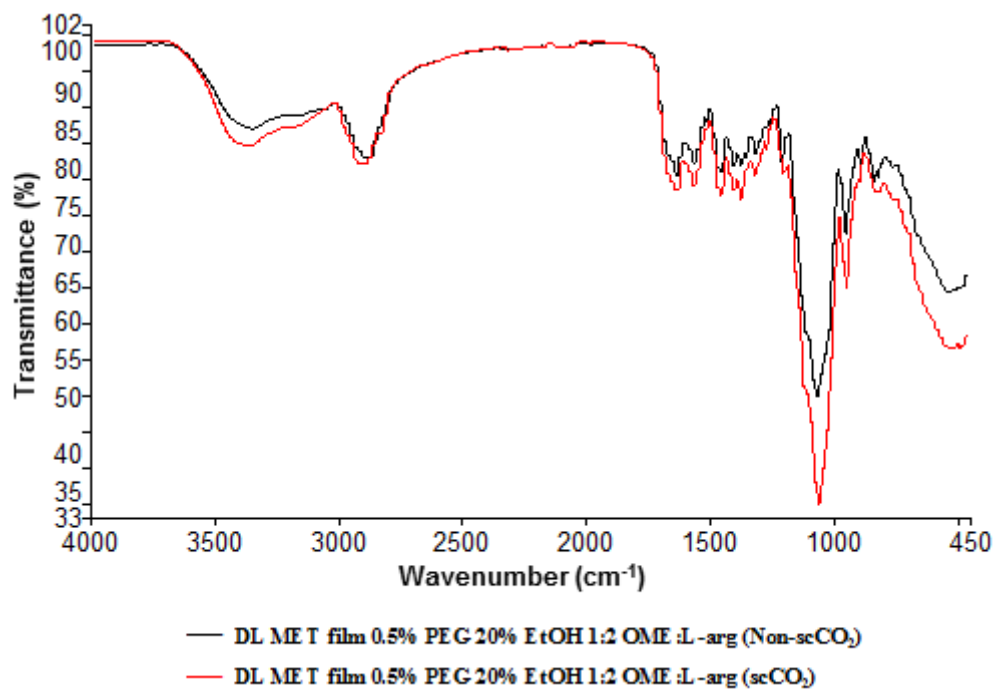


(b)

Figure 5



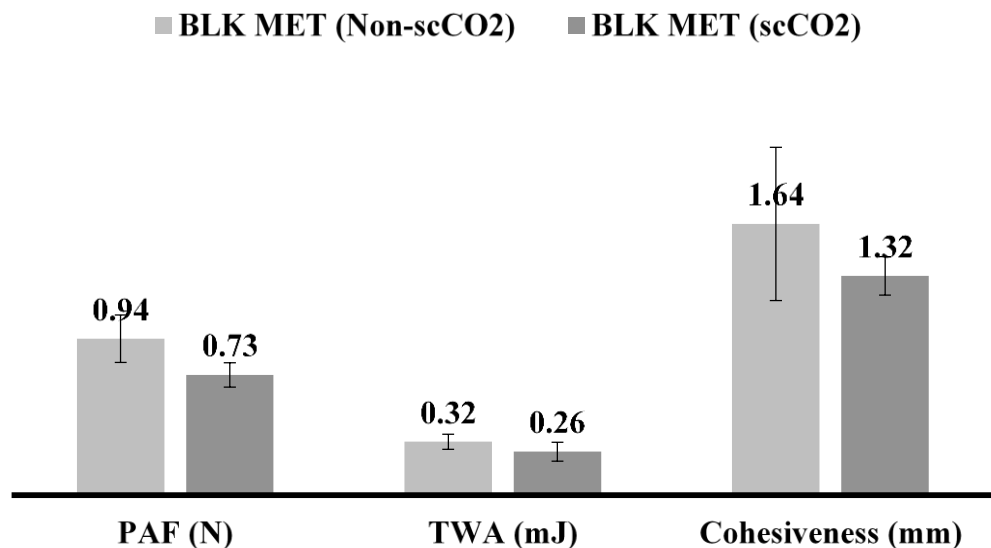
(a)



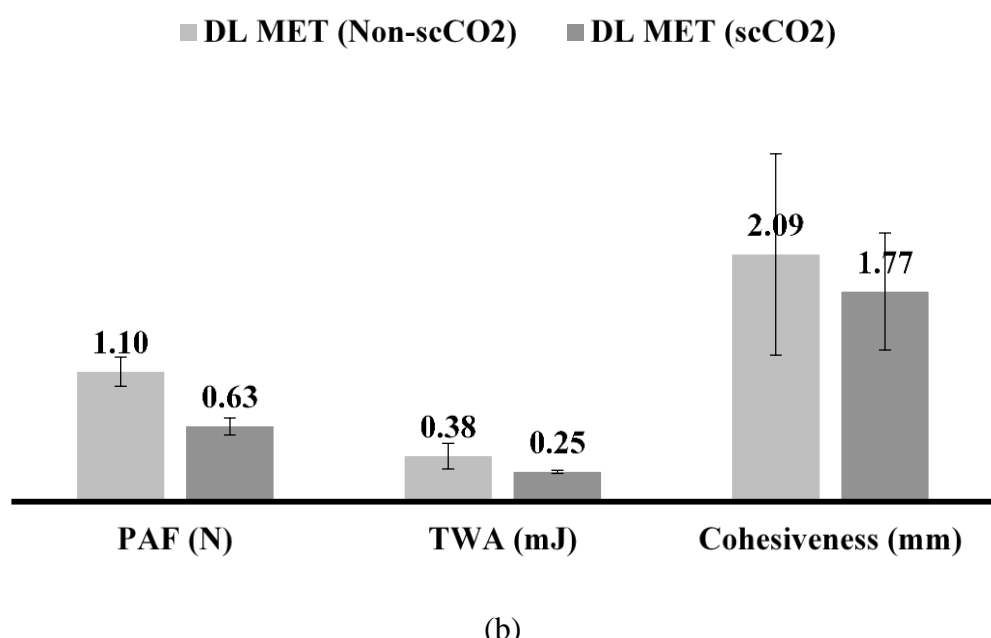
(b)

Figure 6

For colour online and print in black and white



(a)



(b)

Figure 7

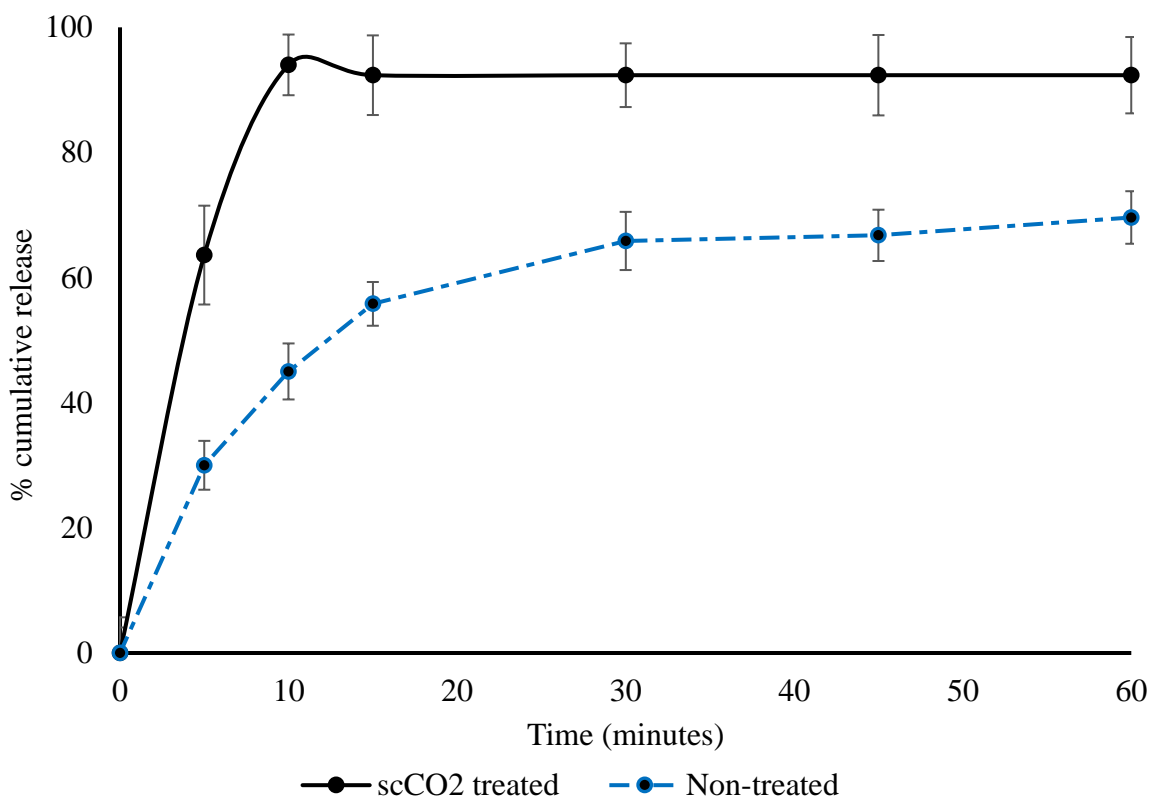


Figure 8